Journal of Physics:
Conference Series

PAPER • **OPEN ACCESS**

Crank–Nicolson Method for the Chiral nonlinear Schrödinger Equation

To cite this article: Ester T. Wahyuningsih *et al* 2025 *J. Phys.: Conf. Ser.* **3114** 012009

Journal of Physics: Conference Series **3114** (2025) 012009 doi:10.1088/1742-6596/3114/1/012009

Crank–Nicolson Method for the Chiral nonlinear Schrödinger Equation

Ester T. Wahyuningsih[1], **I. Magdalena**[1,2,3] **and Canan Akkoyunlu**[4]

[1]Faculty of Mathematics and Natural Sciences, Institut Teknologi Bandung, Indonesia
[2]Center for Coastal and Marine Development, Institut Teknologi Bandung, Indonesia
[3]Center for Mathematical Modelling and Simulations, Institut Teknologi Bandung, Indonesia
[4]Department of Mathematics and Computer Sciences, Istanbul Kültür University, Istanbul, Turkey

E-mail: estertriw16@gmail.com (Ester T. Wahyuningsih), ikha.magdalena@itb.ac.id (Ikha Magdalena). c.kaya@iku.edu.tr (Canan Akkoyunlu)

Abstract. In this paper, we develop a finite difference scheme based on the Crank–Nicolson method for solving the chiral nonlinear Schrödinger (CNLS) equation, which describes the dynamics of nonlinear wave propagation with chirality effects. The CNLS equation supports two types of progressive wave solutions: bright solitons and dark solitons. The proposed Crank–Nicolson scheme is implicit, unconditionally stable, and achieves second-order accuracy in both space and time. To evaluate the accuracy of the method, numerical results are compared with exact analytical soliton solutions. Numerical simulations are presented for the propagation of single bright and dark solitons. The results demonstrate that the Crank–Nicolson method accurately preserves soliton structures, making it an effective tool for studying the dynamics governed by the chiral nonlinear Schrödinger equation. The study demonstrates the effectiveness of the Crank–Nicolson method in capturing the dynamics of chiral nonlinear wave propagation and lays the foundation for further exploration of chiral effects in quantum and optical systems.

1 Introduction

The evolution of wave packets in nonlinear dispersive media is governed by various mathematical models, among which the nonlinear Schrödinger Equation (NLSE) plays a pivotal role due to its wide-ranging applications in optical fibers, plasma physics, deep water waves, and Bose–Einstein condensates [4, 7, 11, 17]. This equation models the balance between dispersive spreading and nonlinear self-interaction, enabling the formation of solitons, localized wave structures that preserve their shape during propagation. Numerous numerical methods, including finite-difference schemes, finite element methods, split-step Fourier techniques, and boundary element methods, have been extensively developed to accurately simulate these nonlinear dynamics [3, 5, 8, 12, 20].

The Chiral nonlinear Schrödinger Equation (CNLS) extends the NLSE by introducing a chiral term, which introduces asymmetry into wave propagation and modifies dispersive behavior [1, 2, 9]. This term alters the conservation of mass, momentum, and energy, therefore, affecting the dynamics and stability of the soliton [14, 21, 22]. In CNLS, soliton propagation depends on both the sign and magnitude of the chiral parameter, bright solitons in self-focusing media and dark solitons in self-defocusing backgrounds propagate in directions influenced by the chiral term [9, 16, 19]. The velocity, width and amplitude of these solitons are tunable by adjusting the amplitude of the wave and the chiral strength of the medium [13]. Exact analytical solutions include sech-type bright solitons and tanh-type dark solitons, which respectively describe localized pulses in self-focusing media and intensity dips in self-defocusing backgrounds. In addition, a variety of optical soliton solutions have been obtained by bifurcation analysis and the Kudryashov method, offering rich insight into the behavior of these nonlinear wave structures [2, 19, 20].

Extensive research has focused on developing the numerical methods for NLSE and CNLS to model soliton interactions [4, 5, 7]. Crank-Nicolson schemes provide second-order accuracy in time and space, ensuring stability in nonlinear dispersive simulations [7, 11, 12]. Other methods, such as FDTD [5], structure-preserving schemes for fractional order models [3], and alternating direction implicit (ADI) compact finite differences [8], are applied to NLSE and CNLS across various dimensions [10, 13]. Studies on multi-soliton dynamics and perturbations deepen understanding of soliton interactions in optical and physical media [16–18]. Recent advances by Bao et al. [7], Gao and Xie [8], and Nauman et al. [10] have enhanced soliton dynamics simulations, while chiral effects have introduced new avenues for exploring asymmetric soliton propagation and multi-soliton interactions [2, 21, 22]. Recent studies on perturbed NLSE models have highlighted the necessity for numerical schemes that efficiently handle derivative nonlinearities and complex wave dynamics [6, 12].

In this work, we propose a linearly implicit Crank-Nicolson scheme for the CNLS, where the dispersive and chiral terms are treated implicitly, while the nonlinear term is handled explicitly. This method allows simulation of bright and dark solitons with dirichlet boundary conditions for the bright solitons, then Robin boundary conditions for the dark solitons [1, 13]. Numerical experiments include one-dimensional, three-dimensional, and surface plots to visualize soliton dynamics in chiral media. The results are compared with analytical solutions derived from previous work, such as sech-type bright solitons, and tanh-type dark solitons, demonstrating that the proposed scheme accurately captures soliton propagation, interaction dynamics, and boundary effects across different soliton types. [10, 18, 19]. This method proves to be a valuable tool for studying nonlinear wave phenomena governed by CNLS, providing both stability and efficiency in complex simulations.

2 Mathematical Model

In this section, we present the Chiral nonlinear Schrödinger (CNLS) equation, which models the evolution of wave packets in a nonlinear, dispersive medium with chiral effects. The CNLS equation enhances the standard NLS by introducing higher-order dispersion and nonlinear terms involving spatial derivatives of the wave function. This formulation captures the combined influence of nonlinearity, dispersion, and chirality, which are essential for accurately describing wave propagation in such media. The final form of the CNLS equation highlights the interplay between spatial and temporal evolution, with terms representing nonlinear self-interaction, dispersion, and chiral contributions. This mathematical formulation provides a comprehensive framework for exploring soliton dynamics and wave interactions influenced by chiral effects. The CNLS equation is expressed as:

$$i\frac{\partial \psi}{\partial t} + \frac{1}{2}\frac{\partial^2 \psi}{\partial x^2} + i\lambda\left(\psi^*\frac{\partial \psi}{\partial x} - \psi\frac{\partial \psi^*}{\partial x}\right)\psi = 0, \quad -\infty < x < \infty, \tag{1}$$

where:

- $\psi(x, t)$ is the complex-valued wave function,
- $\psi^*(x, t)$ denotes the complex conjugate of $\psi(x, t)$,
- λ is a constant that governs the strength of the nonlinear coupling.

This study focuses on the common soliton solutions chosen as initial conditions: the bright soliton, and the dark soliton. Each of these soliton solutions exhibits different characteristics. The bright soliton is a localized wave with a positive amplitude that remains stable over time, while the dark soliton forms a dip in the wave function, creating a localized region of reduced intensity. The subsequent sections will explore these soliton solutions in detail, highlighting their unique properties and their significance in studying nonlinear wave behavior.

2.1 Bright Soliton

The bright soliton is a localized wave solution to the chiral nonlinear Schrödinger equation (CNLS) under the focus of nonlinearity, characterized by a positive nonlinearity parameter $\lambda > 0$. These solitary waveforms emerge because of a precise balance between the dispersive effects of the linear term and

Journal of Physics: Conference Series **3114** (2025) 012009 doi:10.1088/1742-6596/3114/1/012009

the self-focusing effects of the nonlinear term. A Crank-Nicolson finite difference scheme is employed to simulate the time evolution of this bright soliton solution. This method is particularly advantageous because of its unconditional stability, conservation properties, and suitability for handling complex-valued dispersive partial differential equations.
The bright soliton solution to the CNLS equation is given by:

$$\psi(x,t) = A\,\mathrm{sech}\left(\beta(x-ct)\right)\,\exp\left(i(cx+\omega t)\right), \tag{2}$$

when $t = 0$, the initial condition is given by:

$$\psi(x,0) = A\,\mathrm{sech}\left(\beta\left(x-x_0\right)\right), \tag{3}$$

where:

$$\beta = A\sqrt{2\lambda c} \quad \text{and} \quad \omega = \frac{c(2\lambda A^2 - c)}{2}, \tag{4}$$

- A: Amplitude of the soliton,
- β: Inverse width of the soliton,
- c: Velocity of the soliton,
- ω: Wave number.

2.2 Dark Soliton

In contrast, the dark soliton is a solution to the defocusing chiral nonlinear Schrödinger (CNLS) equation, which arises when the nonlinearity parameter is negative $\lambda < 0$. Dark solitons are characterized by localized amplitude depressions within a continuous, non-zero background. Numerical modeling of dark solitons requires careful treatment of boundary conditions, as improper handling may lead to artificial reflections that compromise simulation accuracy. To address this, Robin boundary conditions are implemented to effectively accommodate the background phase gradient and ensure stable soliton propagation within the computational domain.
The dark soliton solution to the CNLS equation is given by:

$$\psi(x,t) = A\tanh\left(\beta(x-ct)\right)\exp\left(i(cx+\omega t)\right), \tag{5}$$

when $t = 0$, the initial condition is given by:

$$\psi(x,0) = A\tanh\left(\beta(x-x_0)\right), \tag{6}$$

where:

$$\beta = A\sqrt{-2\lambda c} \quad \text{and} \quad \omega = \frac{c(4\lambda A^2 - c)}{2}, \tag{7}$$

- A: Amplitude of the soliton,
- β: Inverse width of the soliton,
- c: Velocity of the soliton,
- ω: Wave number.

3 Numerical Solution

In this section, the numerical method used to solve the Chiral nonlinear Schrödinger (CNLS) equation is described. The equation is discretized in both spatial and temporal domains using a finite difference method combined with the Crank–Nicolson time-stepping scheme. This implicit scheme offers second-order accuracy in both space and time and provides unconditional stability for linear problems, making it well-suited for simulating the CNLS equation.

3.1 Discretization of the Domain

Let the spatial domain $[a, b]$ be divided into N uniform grid points with spacing

$$\Delta x = \frac{b-a}{N-1}, \tag{8}$$

and the time domain $[0, T]$ be discretized into M steps with time step

$$\Delta t = \frac{T}{M}. \tag{9}$$

We denote the discrete spatial points by

$$x_j = a + j\Delta x, \quad \text{for } j = 0, 1, 2, \ldots, N-1, \tag{10}$$

and discrete time levels by

$$t_n = n\Delta t, \quad \text{for } n = 0, 1, 2, \ldots, M. \tag{11}$$

The approximate solution at point (x_j, t_n) is denoted by

$$\psi_j^n \approx \psi(x_j, t_n). \tag{12}$$

3.2 Finite Difference Approximation

The spatial and temporal derivatives in the CNLS equation are approximated using finite difference formulas:

- The second-order spatial derivative is approximated by a central difference:

$$\left.\frac{\partial^2 \psi}{\partial x^2}\right|_j^n \approx \frac{\psi_{j+1}^n - 2\psi_j^n + \psi_{j-1}^n}{(\Delta x)^2}. \tag{13}$$

- The first-order temporal derivative is approximated using the Crank-Nicolson method, which averages the spatial derivatives at two successive time levels:

$$\left.\frac{\partial \psi}{\partial t}\right|_j^{n+\frac{1}{2}} \approx \frac{\psi_j^{n+1} - \psi_j^n}{\Delta t}. \tag{14}$$

- The nonlinear term $|\psi|^2\psi$ is evaluated explicitly at time level n, avoiding nonlinear iterations.

It is worth noting that the Crank–Nicolson scheme is unconditionally stable for linear problems, making it a robust choice for solving the CNLS equation, which involves a linear dispersive term combined with a nonlinear interaction term.

3.3 Semi-Implicit Crank–Nicolson Scheme Formulation

We adopt a Crank–Nicolson scheme to numerically integrate the CNLS equation. The linear dispersive term is discretized using a second-order central difference and treated implicitly, while the nonlinear term is evaluated explicitly at the current time level. This choice avoids solving nonlinear systems at each time step and maintains computational efficiency.

The semi-discrete form of the CNLS equation is written as:

$$\frac{\psi^{n+1} - \psi^n}{\Delta t} = \frac{i}{2}\left(L\psi^{n+1} + L\psi^n\right) + i\lambda|\psi^n|^2\psi^n, \tag{15}$$

where ψ^n and ψ^{n+1} are the numerical approximations of the wavefunction at time levels t_n and t_{n+1}, respectively. The operator L denotes the discrete second-order spatial derivative matrix, constructed using the central difference scheme, and λ is the nonlinear coefficient. All operations are carried out directly in the complex domain without decomposition into real and imaginary parts, leveraging the native support for complex arithmetic.

Journal of Physics: Conference Series **3114** (2025) 012009 doi:10.1088/1742-6596/3114/1/012009

Rearranging the equation, we obtain the linear system to solve at each time step:

$$A\psi^{n+1} = B\psi^n + i\Delta t\, N(\psi^n), \tag{16}$$

with:

$$A = I + \frac{i\Delta t}{2}L, \qquad B = I - \frac{i\Delta t}{2}L, \tag{17}$$

where I is the identity matrix, and $N(\psi^n) = \lambda|\psi^n|^2\psi^n$ represents the nonlinear interaction evaluated explicitly.

This semi-implicit approach preserves the favorable stability properties of the Crank–Nicolson method for the linear part while avoiding the complexity of solving nonlinear systems. It provides a good balance between computational efficiency and accuracy, especially in long-time soliton simulations.

3.4 Treatment of the Complex-Valued and Nonlinear Terms

In this study, the CNLS equation is solved directly in its complex-valued form without decomposition into real and imaginary components. This approach simplifies implementation and improves computational efficiency, as modern numerical computing environments natively support complex arithmetic

The cubic nonlinear term $|\psi|^2\psi$ is evaluated explicitly at each time level as

$$N(\psi^n)_j = \lambda|\psi_j^n|^2\psi_j^n, \tag{18}$$

and incorporated into the right-hand side of the Crank–Nicolson scheme. By treating the nonlinearity explicitly, the resulting linear system can be solved efficiently at each time step without requiring nonlinear iterations, thereby improving computational stability and performance.

Although the chiral term does not appear explicitly in the finite difference formulation, its physical influence is embedded through the parameter λ and the initial condition derived from the analytical soliton profile. This ensures that the simulated waveforms accurately capture the dynamics induced by the chiral interaction. Overall, the combination of complex-valued arithmetic and explicit nonlinear treatment provides a robust, efficient, and physically consistent numerical framework for simulating chiral soliton dynamics.

3.5 Boundary Conditions

To complete the numerical formulation, appropriate boundary conditions are applied to the spatial domain boundaries. In this study, different types of boundary conditions are employed depending on the type of soliton solution considered:

- For the bright soliton solution, homogeneous Dirichlet boundary conditions are imposed:

  $$\psi(a,t) = \psi(b,t) = 0, \quad \text{for all } t \in [0,T] \tag{19}$$

  This choice is suitable because bright solitons are localized structures that rapidly decay to zero as $x \to \pm\infty$. Thus, enforcing zero Dirichlet boundaries at sufficiently far domain endpoints introduces negligible error and prevents artificial reflections.

- For the dark soliton solution, homogeneous Robin boundary conditions are applied:

  $$\frac{\partial\psi}{\partial x}(a,t) = \frac{\partial\psi}{\partial x}(b,t) = 0, \quad \text{for all } t \in [0,T] \tag{20}$$

  This choice is appropriate for dark solitons, characterized by a localized intensity dip propagating over a constant nonzero background. In contrast to Dirichlet conditions, Robin boundary conditions help preserve this background and allow the soliton to evolve naturally, minimizing spurious reflections and boundary-induced distortions in amplitude or phase.

These boundary conditions ensure the well-posedness of the problem and are consistent with the physical behavior of the respective soliton types.

4 Results and Discussion

In this section, we present and analyze the results of numerical simulations performed for the Chiral nonlinear Schrödinger equation (CNLS) using the Crank-Nicolson finite difference scheme. The aim is to investigate the propagation dynamics, stability, and interaction characteristics of different soliton solutions, there are the bright soliton, the dark soliton, and the interaction of two bright solitons.

4.1 Bright Soliton

The simulation of the bright soliton was conducted using the initial condition defined in Equation (3) and Dirichlet Boundary Condition in Equation (19) with parameters :

$$x_L = -50.0, \quad x_R = 50.0, \quad h = 0.05, \quad k = 0.01$$

$$A = 0.5, \quad \lambda = 0.5, \quad v = 0.5, \quad t = 0, 1, 2, \ldots, 20$$

To visualize the evolution of the wave, we present three different plots: a one-dimensional (1D) line plot showing the profile at multiple time levels, a three-dimensional (3D) plot to illustrate the time-space evolution, and a 3D surface plot with color mapping to highlight the amplitude distribution. These visualizations help us interpret the qualitative behavior of the soliton and assess the stability of the numerical scheme.

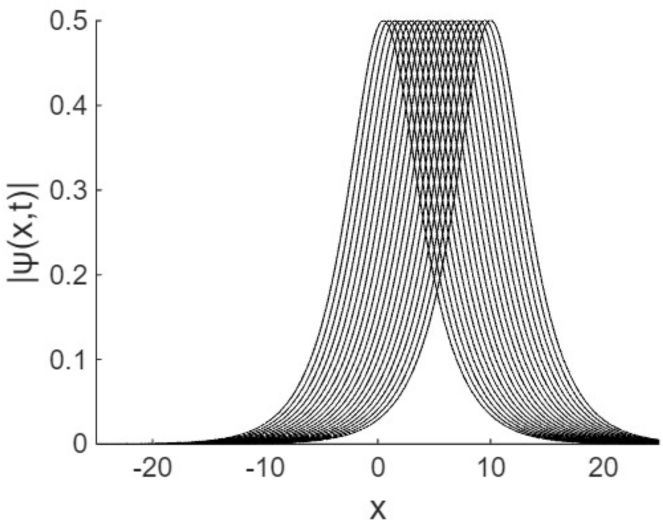

Figure 1: One-dimensional profiles of the bright soliton at $t \in [0, 20]$ for parameters $x_L = -50$, $x_R = +50$, $h = 0.05$, $k = 0.01$, $A = 0.5$, $\lambda = 0.5$, $v = 0.5$. This figure shows preservation of amplitude and shape over propagation.

Figure 1 shows a one-dimensional line plot of $|\psi(x,t)|$ for multiple time steps. The amplitude remains approximately $A = 0.5$, with no noticeable decay or oscillation, indicating the effectiveness of the numerical scheme in conserving the structural integrity of the soliton. This confirms the localized and stable nature of the bright soliton solution, where the nonlinear self-focusing perfectly balances dispersive spreading.

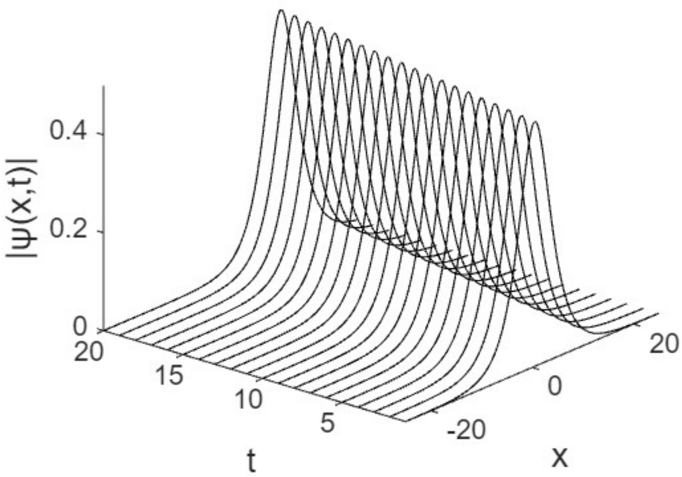

Figure 2: Wireframe plot of $|\psi(x,t)|$ for the bright soliton at $t \in [0,\, 20]$ with parameters $x_L = -50$, $x_R = +50$, $h = 0.05$, $k = 0.01$, $A = 0.5$, $\lambda = 0.5$, $v = 0.5$. This illustrates the constant-amplitude ridge moving at velocity v without dispersion.

Figure 2 illustrates a wireframe plot 3D visualization of $|\psi(x,t)|$ of the bright soliton. It's representations demonstrate the characteristic behavior of the soliton; its amplitude remains constant while propagating in time without dispersion. In the wireframe plot (Figure 2), the soliton peak moves consistently along the spatial axis x as time t increases, reflecting a motion to the right. The sharp and consistent peak profile confirms the stability of the soliton and its resistance to deformation.

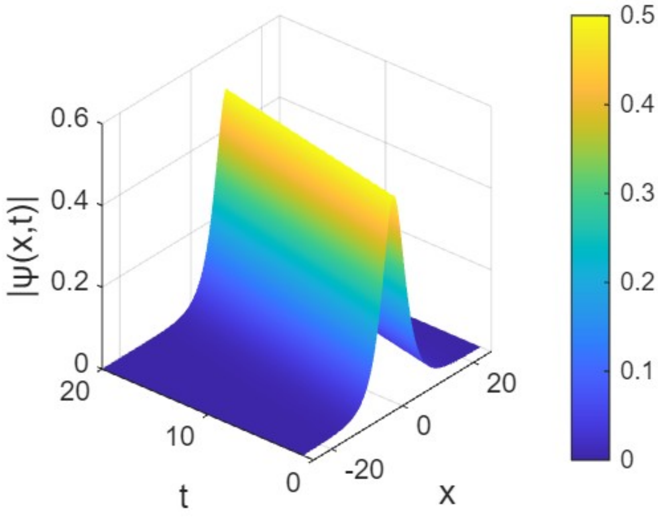

Figure 3: Surface (color-mapped) view of bright-soliton amplitude for $x_L = -50$ to $+50$, $t \in [0,\, 20]$ with parameters $x_L = -50$, $x_R = +50$, $h = 0.05$, $k = 0.01$, $A = 0.5$, $\lambda = 0.5$, $v = 0.5$. Color indicates $|\psi|$, highlighting energy conservation and absence of boundary reflections under Dirichlet boundary conditions.

Meanwhile, the surface plot (Figure 3) offers a smooth, color-coded representation of the dynamics, clearly illustrating the amplitude distribution. The yellow ridge corresponds to the maximum amplitude at the crest $A = 0.5$, which remains constant throughout the simulation, reinforcing the conclusion that the soliton preserves its energy and shape. The application of homogeneous Dirichlet boundary conditions ensures that spurious reflections are effectively prevented by the boundary setup.

To validate the numerical model, the bright soliton profile obtained from the numerical simulation was compared with the exact analytical solution at $t = 10$. Figure 4 presents the comparison between the numerical and analytical solutions.

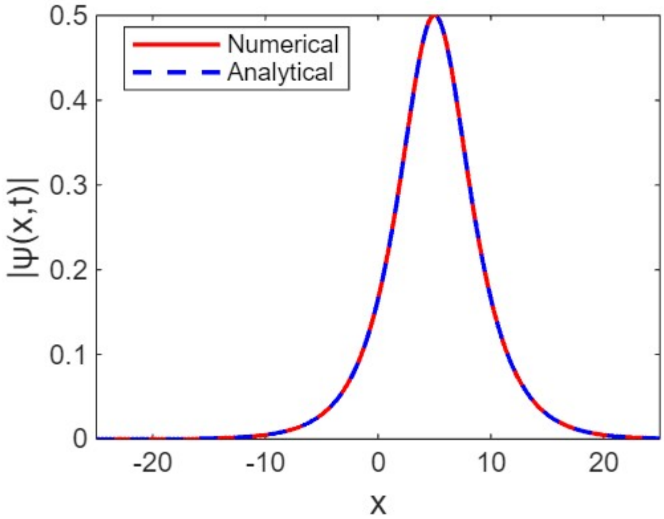

Figure 4: Comparison of numerical and analytical bright soliton at $t = 10$, with $h = 0.05$, $k = 0.01$.

As shown in Figure 4, the numerical solution closely matches the analytical profile in both amplitude and position, maintaining the expected peak at approximately $A = 0.5$. Furthermore, the root mean square error (RMSE) between the numerical and analytical solutions at $t = 10$ was calculated to be 6.5062×10^{-5}, indicating a high level of agreement. The overlay comparison plot confirms that the Crank–Nicolson scheme accurately captures the soliton shape and propagation without noticeable deformation, further validating the reliability and stability of the numerical method.

The simulation of the bright soliton evolution was executed on a standard consumer laptop (Intel Core i3-1115G4 @ 3.00GHz, 4 GB RAM), requiring approximately 8.29 seconds of CPU time. The scheme is linearly implicit, avoiding nonlinear iterations, making it highly efficient for long-time integration with minimal computational resources.

4.2 Dark Soliton

The dark soliton simulation was performed using the initial condition defined in Equation (6) and Robin boundary condition in Equation (20) with parameters :

$$x_L = -50.0, \quad x_R = 50.0, \quad h = 0.05, \quad k = 0.001$$

$$A = 0.5, \quad \lambda = -0.5, \quad c = 0.5, \quad t = 0, 1, 2, \ldots, 20$$

To capture the dynamics of the dark soliton, we present three types of visualizations: a one-dimensional (1D) line plot, a three-dimensional (3D) wireframe plot, and a 3D surface plot with colormap enhancement. These graphical representations allow a qualitative analysis of the soliton's profile, stability, and motion characteristics.

Figure 5 shows the amplitude $|\psi(x, t)|$ of the dark soliton at different time steps. Unlike bright solitons, dark solitons feature a characteristic dip (notch) in the amplitude, which propagates without altering its depth or width, indicating the balance between dispersion and nonlinearity. The Crank–Nicolson method preserves the soliton's shape with no significant spreading or loss of amplitude, indicating high stability. Additionally, the absence of spurious reflections at the boundaries confirms the proper implementation of the Robin boundary conditions, ensuring accurate soliton propagation.

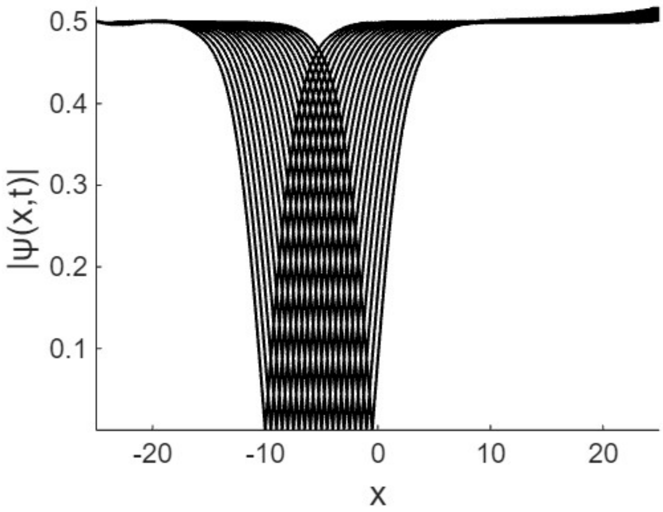

Figure 5: One-dimensional profiles of the dark soliton at $t \in [0,\, 20]$ for parameters $x_L = -50$, $x_R = +50$, $h = 0.05$, $k = 0.001$, $A = 0.5$, $\lambda = -0.5$, $c = 0.5$. Demonstrates stable notch propagation without amplitude loss.

Next, we present a 3D plot of the dark soliton evolution which further demonstrates how the soliton's shape is consistently maintained across the simulation domain. Figure 6 illustrates the three-dimensional evolution of the dark soliton. The characteristic notch in the amplitude $|\psi(x,t)|$ remains sharp and stable throughout the simulation, with no significant dispersion or deformation. This clearly demonstrates the balance between nonlinear and dispersive effects, ensuring the soliton consistently preserves its profile as it propagates. The result further confirms the Crank–Nicolson method's accuracy and robustness in simulating dark soliton dynamics within the CNLS framework.

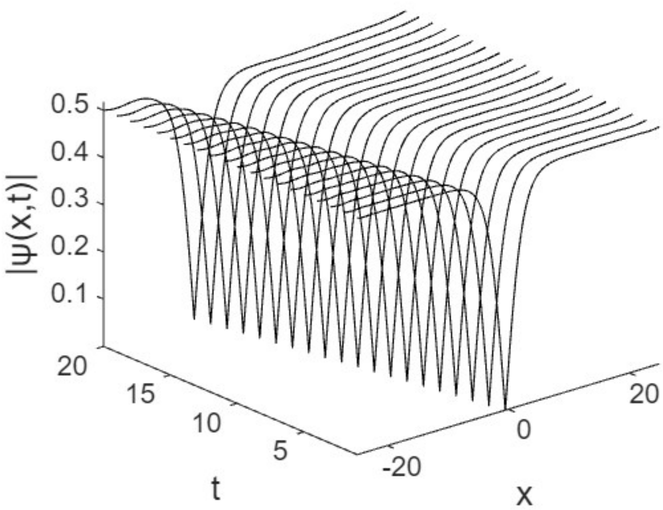

Figure 6: Wireframe plot of $|\psi(x,t)|$ for the dark soliton at $t \in [0,\, 20]$ with parameters $x_L = -50$, $x_R = +50$, $h = 0.05$, $k = 0.001$, $A = 0.5$, $\lambda = -0.5$, $c = 0.5$. Highlights the persistent localized dip (notch) traveling at constant speed.

For a more comprehensive depiction of the dark soliton's spatiotemporal amplitude evolution, Figure 7 presents a surface plot with a continuous color mapping. This visualization effectively captures the localized intensity dip as a pronounced blue trough, corresponding to the soliton's "notch", while the uniform yellow regions represent the constant background field, emphasizing the contrast between the soliton core and the surrounding medium.

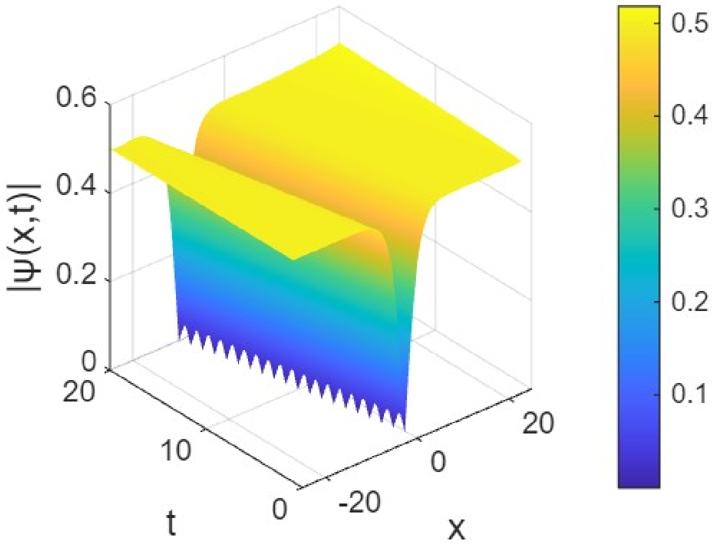

Figure 7: Surface (colormap) representation of dark-soliton amplitude showing the localized amplitude for $x_L = -50$ to $+50$, $t \in [0, 20]$ with parameters $x_L = -50$, $x_R = +50$, $h = 0.05$, $k = 0.001$, $A = 0.5$, $\lambda = -0.5$, $c = 0.5$

The results demonstrate that the Crank–Nicolson scheme is highly effective for simulating dark solitons under defocusing nonlinearity. The numerical method accurately captures the evolution of the soliton's structure, ensuring that its characteristic features are maintained throughout the simulation.

To assess the accuracy of the numerical model, the dark soliton profile obtained from the simulation was compared with the exact analytical solution at $t = 10$. Figure 8 illustrates this comparison. These results demonstrate the robustness and reliability of the proposed method for simulating nonlinear wave phenomena governed by the CNLS equation.

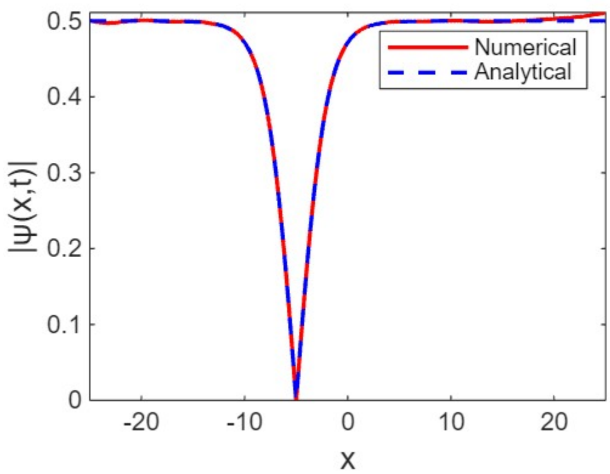

Figure 8: Overlay of numerical and analytical $|\psi(x, t)|$ at $t = 10$. for $h = 0.05$, $k = 0.001$, confirming reliability of the scheme under Robin boundary conditions.

As shown in Figure 8, the numerical solution shows good agreement with the analytical profile in both amplitude and shape. The root mean square error (RMSE) is 2.21×10^{-3}, indicating a satisfactory level of accuracy. The soliton dip remains at the expected position, with no significant deformation or phase shift. The overlay plot confirms that the Crank–Nicolson scheme accurately captures the dark soliton dynamics, validating the method's stability and precision.

For the dark soliton case, the numerical simulation completed in approximately 6.00 seconds on the a standard consumer laptop (Intel Core i3-1115G4 @ 3.00GHz, 4 GB RAM). The semi-implicit Crank–Nicolson scheme combined with Robin boundary conditions enables stable and accurate resolution of soliton dynamics without significant computational cost.

4.3 Numerical Accuracy, Convergence, and Stability Analysis

To evaluate the performance of the proposed Crank-Nicolson scheme, we performed a detailed analysis of its numerical accuracy, convergence behavior, and stability properties for both the bright and dark soliton solutions of the CNLS equation.

RMSE Analysis.

To quantitatively assess the accuracy of the proposed Crank–Nicolson scheme, the Root Mean Square Error (RMSE) between the analytical and numerical solutions was computed over the simulation time. The evolution of RMSE values for both bright and dark solitons is presented in Table 1. As expected, bright solitons exhibited consistently lower RMSE values due to their simpler localized structure, while dark solitons showed slightly higher errors attributed to their constant background and localized dip.

Table 1: RMSE values of bright and dark solitons at selected time points.

Time (t)	**Bright Soliton RMSE**	**Dark Soliton RMSE**
1	2.46×10^{-5}	2.38×10^{-4}
5	4.34×10^{-5}	1.08×10^{-3}
10	6.51×10^{-5}	2.21×10^{-3}
15	9.05×10^{-5}	3.41×10^{-3}
20	1.21×10^{-4}	4.62×10^{-3}

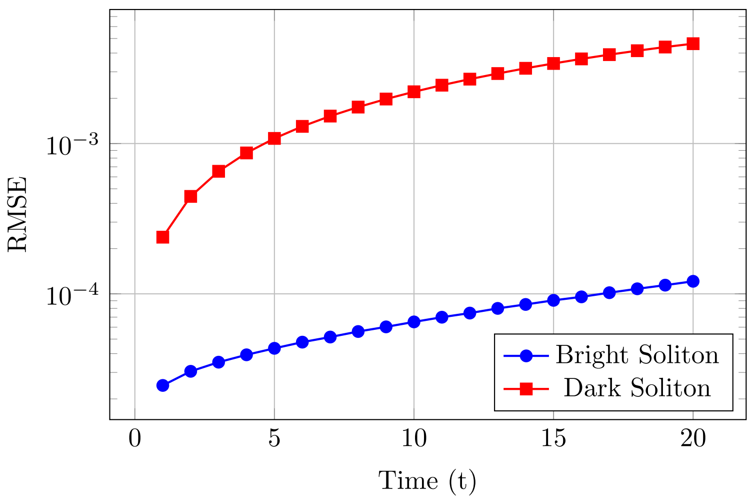

Figure 9: Comparison plot of RMSE versus time for bright soliton at $h = 0.05$ and $k = 0.01$. and dark solitons at $h = 0.05$ and $k = 0.001$. Quantifies overall accuracy and reveals dark-soliton error growth trend over time.

The RMSE analysis presented in Figure 9 provides a comprehensive assessment of the numerical scheme's accuracy over time for both bright and dark soliton cases. The results clearly indicate that the bright solitons maintain consistently lower RMSE values due to their localized structure and the use of Dirichlet boundary conditions, which limit boundary interactions and numerical dispersion. This can be attributed to the Dirichlet boundary conditions and the inherent localized nature of bright solitons, which minimize interactions with the computational domain boundaries and reduce cumulative numerical errors. In contrast, dark soliton simulations exhibit higher RMSE with a gradual increase over time. This trend is attributed to the constant background field and localized intensity dip, which are more sensitive to discretization and boundary effects, particularly under Robin boundary conditions. Despite these differences, both soliton types demonstrate acceptable error levels, confirming that the Crank–Nicolson scheme effectively preserves the soliton profiles and dynamics for chiral nonlinear Schrödinger equation soliton simulations.

Convergence Analysis

To assess the spatial accuracy of the Crank–Nicolson discretization, we performed a grid refinement study by computing the RMSE between the numerical and analytical solutions at $t = 10$. Simulations were conducted for decreasing spatial step sizes $h = \{0.4, 0.2, 0.1, 0.05, 0.025\}$, with the time step k scaled proportionally to h^2 to suppress temporal discretization errors and isolate spatial convergence behavior.

Table 2: RMSE values at $t = 10$ for different grid resolutions.

h	Bright Soliton RMSE	Dark Soliton RMSE
0.400	2.27×10^{-4}	1.36×10^{-2}
0.200	5.77×10^{-5}	6.30×10^{-3}
0.100	1.57×10^{-5}	3.12×10^{-3}
0.050	5.79×10^{-6}	1.56×10^{-3}
0.025	3.89×10^{-6}	7.76×10^{-4}

Table 2 reports the RMSE values obtained at $t = 10$ for various spatial step sizes h, confirming the convergence behavior of the proposed scheme. As h decreases, the RMSE consistently decreases for both bright and dark soliton cases, indicating that the numerical solution converges to the exact solution.

In the bright soliton case, the error decreases rapidly with finer grids, and the local convergence order approaches two. This behavior aligns with the expected second-order accuracy of the Crank–Nicolson method. The high accuracy is further supported by the localized structure of the bright soliton and the use of homogeneous Dirichlet boundary conditions, which effectively minimize boundary-induced errors.

In contrast, the dark soliton simulations exhibit a convergence rate that stabilizes around first-order. This reduced accuracy is primarily attributed to the presence of a non-zero background field combined with a localized intensity dip at the soliton core. Such a structure introduces steep gradients and a sharp transition zone, which are more difficult to resolve accurately on coarse grids. Moreover, the use of Robin boundary conditions amplifies boundary sensitivity, limiting global error reduction, especially at finer resolutions. Despite these challenges, the numerical results remain stable and sufficiently accurate for capturing the essential features of dark soliton dynamics.

Stability Analysis.

To assess the numerical stability of the Crank–Nicolson scheme under varying nonlinear strengths and time resolutions, we varied the nonlinearity coefficient $\lambda \in \{0.1,\ 0.5,\ 1.0,\ 2.0,\ 5.0\}$ and tested time step sizes $k \in \{0.001,\ 0.005,\ 0.01,\ 0.02,\ 0.05\}$, with a fixed spatial step $h = 0.05$.

Table 3: Stability results for bright and dark solitons with different λ and time step k. A value of '1' denotes stability; '0' indicates instability.

λ	Bright Soliton					Dark Soliton				
	$k = 0.001$	0.005	0.01	0.02	0.05	$k = 0.001$	0.005	0.01	0.02	0.05
0.1	1	1	1	1	1	1	1	1	1	1
0.5	1	1	1	1	1	1	1	1	1	1
1.0	1	1	1	1	1	1	1	1	1	1
2.0	1	1	1	1	1	1	1	1	1	0
5.0	1	1	1	1	1	0	0	0	0	0

For bright solitons ($\lambda > 0$), the scheme remained stable across all configurations, including large nonlinearities and time steps. This robustness reflects the unconditional stability of the Crank–Nicolson

Journal of Physics: Conference Series **3114** (2025) 012009 doi:10.1088/1742-6596/3114/1/012009

method, aided by the localized nature of bright solitons and Dirichlet boundary conditions that mitigate spurious reflections.

For dark solitons ($\lambda < 0$), stability was maintained for moderate nonlinearities ($\lambda \leq 2.0$) with sufficiently small time steps. However, instability emerged at $\lambda = 2.0$ for $k = 0.05$, and across all time steps for $\lambda = 5.0$. The reduced stability is attributed to the non-zero background, steep gradients near the soliton core, and the use of Robin boundary conditions—all of which amplify sensitivity to temporal resolution. Despite this, the method remains reliable for dark solitons under controlled time stepping.

4.4 Method Comparison.

Various numerical approaches have been proposed to solve the chiral nonlinear Schrödinger (CNLS) equation, including finite difference schemes with real–imaginary splitting and method of lines (MOL) formulations. The scheme in [1] employs a Crank–Nicolson discretization after decomposing the CNLS equation into real and imaginary parts. While this approach ensures conservation properties, it introduces additional algebraic complexity and coupling between components. In this work, we adopt a direct complex-valued formulation that eliminates the need for splitting, enabling a more compact implementation while leveraging modern solvers' native support for complex arithmetic. This simplifies the numerical treatment and contributes to improved computational efficiency.

In [15], the authors employ a method-of-lines (MOL) approach, combined with explicit Runge–Kutta and predictor–corrector time integration schemes. While these methods are capable of achieving accurate results and are relatively straightforward to implement, they are inherently limited by stability constraints, particularly in stiff regimes. As a result, small time steps are often required to maintain numerical stability, which can increase computational cost. In contrast, the Crank–Nicolson scheme used in this work is linearly implicit and unconditionally stable, enabling the use of larger time steps and facilitating efficient long-time integration, even on coarse spatial grids and limited computational cost. Overall, the proposed scheme offers a balanced trade-off between stability, accuracy, and computational cost, making it a practical and robust alternative for simulating soliton dynamics in the CNLS framework.

5 Conclusion

In this study, we introduced a linearly implicit Crank-Nicolson scheme for the numerical simulation of the Chiral nonlinear Schrödinger Equation (CNLS), successfully applied to the dynamics of bright soliton and dark soliton. The Crank-Nicolson method, which discretizes the dispersive and chiral terms implicitly while treating the nonlinear term explicitly, proved to be an effective tool for simulating soliton propagation with high stability and accuracy.

For the bright soliton, the numerical simulations showed excellent preservation of the soliton's amplitude and shape, with no noticeable dispersion or loss of energy. The comparison with the exact analytical solution at t=10 confirmed the accuracy, precision and stability of the numerical scheme. Similarly, the dark soliton simulations demonstrated the effective handling of the soliton's characteristic "notch" structure, maintaining its stability and velocity without deformation or dispersion, in line with the exact solution. Additionally, the use of Dirichlet boundary conditions for the bright soliton and Robin boundary conditions for the dark soliton helped prevent spurious reflections, ensuring that the numerical model remained stable and accurate throughout the simulations. The presented 1D, 3D, and surface plots effectively illustrated the soliton dynamics and validated the robustness of the Crank-Nicolson scheme for the types of solitons.

To rigorously assess numerical performance, we conducted convergence and stability tests. A grid refinement study demonstrated that the method achieves second-order accuracy for bright solitons and first-order convergence for dark solitons, consistent with the presence of a non-zero background. Stability tests across a range of nonlinearity coefficients and time steps confirmed that the scheme remains robust under moderate to strong nonlinear effects, especially when suitable time-stepping is employed.

In conclusion, the proposed numerical method is a reliable and efficient approach for simulating soliton dynamics in nonlinear Schrödinger equations, capable of accurately capturing the essential features of soliton propagation while preserving their energy and structure. Unlike previous works that rely on real–imaginary decomposition or iterative solvers, our method directly solves the CNLS equation in its complex-valued form with a linearly implicit Crank–Nicolson scheme. This approach not only simplifies implementation but also improves computational efficiency, especially for long-time integration. Furthermore, we demonstrate its robust applicability to both bright and dark solitons by incorporating tailored boundary conditions (Dirichlet and Robin) that minimize numerical artifacts. Future work could extend this approach to more complex configurations, including multi-soliton interactions or higher-dimensional systems.

References

[1] Ismail M S, Al-Basyouni K S, and Aydin A 2015 Conservative finite difference schemes for the chiral nonlinear Schrödinger equation *Boundary Value Problem* **2015** 89
https://doi.org/10.1186/s13661-015-0350-4

[2] Alkahtani B S T 2025 Propagation of wave insights to the chiral Schrödinger equation along with bifurcation analysis and diverse optical soliton solutions *Alexandria Engineering Journal* **108** 800–810
https://doi.org/10.1016/j.aej.2024.08.116

[3] Hu D, Gong Y, and Wang Y 2021 On convergence of a structure preserving difference scheme for two-dimensional space-fractional nonlinear Schrödinger equation and its fast implementation *Computers and Mathematics with Applications* **98** 10–23
https://doi.org/10.1016/j.camwa.2021.06.018

[4] Chang Q, Jia E, and Sun W 1999 Difference schemes for solving the generalized nonlinear Schrödinger equation *J. Comput. Phys.* **148** 397–415
https://doi.org/10.1006/jcph.1998.6120

[5] Moxley F I, Chuss D T, and Dai W 2013 A generalized finite-difference time-domain scheme for solving nonlinear Schrödinger equations *Computer Physics Communications* **184** 1834–1841
https://doi.org/10.1016/j.cpc.2013.03.006

[6] Bian S P Y and Guo B 2022 Numerical simulation of a generalized nonlinear derivative Schrödinger equation *Electronic Research Archive* **30**(8) 3130–3152
https://doi.org/10.3934/era.2022159

[7] Bao W, Tang Q, and Xu Z 2012 Numerical methods and comparison for computing dark and bright solitons in the nonlinear Schrödinger equation *Journal of Computational Physics* **235** 423–445
https://doi.org/10.1016/j.jcp.2012.10.054

[8] Gao Z and Xie S 2010 Fourth-order alternating direction implicit compact finite difference schemes for two-dimensional Schrödinger equations *Applied Numerical Mathematics* **61** 593–614
https://doi.org/10.1016/j.apnum.2010.12.004

[9] Nishino A, Umeno Y, and Wadati M 1998 Chiral nonlinear Schrödinger Equation *Chaos, Solitons & Fractals* **9** 1063–1069
https://doi.org/10.1016/S0960-0779(97)00184-7

[10] Raza N R and Arshed S 2020 Chiral bright and dark soliton solutions of Schrödinger's equation in (1 + 2)-dimensions *Ain Shams Engineering Journal* **11** 1237–1241
https://doi.org/10.1016/j.asej.2020.03.018

[11] Arora G, Rani R, and Emadifar H 2022 Numerical solutions of nonlinear Schrödinger equation with applications in optical fiber communication *Optik* **266** 169661
https://doi.org/10.1016/j.ijleo.2022.169661

[12] Le A H, Huynh T, and Nguyen Q M 2024 Analysis of a Crank–Nicolson finite difference scheme for (2 + 1)D perturbed nonlinear Schrödinger equations with saturable nonlinearity *Computers and Mathematics with Applications* **167** 160–177
https://doi.org/10.1016/j.camwa.2024.05.015

[13] Awan A U, Tahir M, and Abro K A 2021 Multiple soliton solutions with chiral nonlinear Schrödinger's equation in (2+1)-dimensions *European Journal of Mechanics / B Fluids* **85** 68–75
https://doi.org/10.1016/j.euromechflu.2020.07.014

[14] Torres-Silva H and Zamorano M 2003 Chiral effects on optical solitons *Mathematics and Computers in Simulation* **62** 149–161
https://doi.org/10.1016/S0378-4754(02)00177-5

[15] Al-Basyouni K S and Ismail M S 2009 Method of Lines for the Chiral nonlinear Schrödinger Equation *Nuclear Physics B* **806** 457–461
https://doi.org/10.1016/j.nuclphysb.2008.05.023

[16] Biswas A 2009 Perturbation of chiral solitons *Applied Mathematics* **11** 447–459 https://doi.org/10.4236/am.2020.116032

[17] Ahmad J, Rani S, Turki N B, and Shah N A 2023 Novel resonant multi-soliton solutions of time fractional coupled nonlinear Schrödinger equation in optical fiber via an analytical method *Results in Physics* **52** 106761 https://doi.org/10.1016/j.rinp.2023.106761

[18] Sahar A, Mohammed W W, Aiyashi M A, and Abdelrahman M A E 2020 Exact Solutions of the (2 + 1)-Dimensional Stochastic Chiral nonlinear Schrödinger Equation *Symmetry* https://doi.org/10.3390/sym12111874

[19] Aly E S, Abdelrahman M A E, Bourazza S, Ahmadini A A H, Msmali A H, and Askar N A 2020 New solutions for perturbed chiral nonlinear Schrödinger equation *AIMS Mathematics* **7** 12289–12302 https://doi.org/10.3934/math.2022682

[20] Alshahrani B, Yakout H A, Khater M M A, Abdel-Aty A H, Mahmoud E E, Baleanu D, and Eleuch H 2021 Accurate novel explicit complex wave solutions of the (2+1)-dimensional Chiral nonlinear Schrödinger equation *Results in Physics* **23** 104019 https://doi.org/10.1016/j.rinp.2021.104019

[21] Wang K and Wang G 2021 Variational theory and new abundant solutions to the (1+2)-dimensional chiral nonlinear Schrödinger equation in optics *Physics Letters A* **412** 127588 https://doi.org/10.1016/j.physleta.2021.127588

[22] Al Woadud K M A, Kumar D, and Khan A R 2023 Obliquely propagating optical wave patterns to the (2 + 1)-dimensional chiral nonlinear Schrödinger equation in the absence and presence of Atangana derivative *Results in Physics* **54** 107113 https://doi.org/10.1016/j.rinp.2023.107113